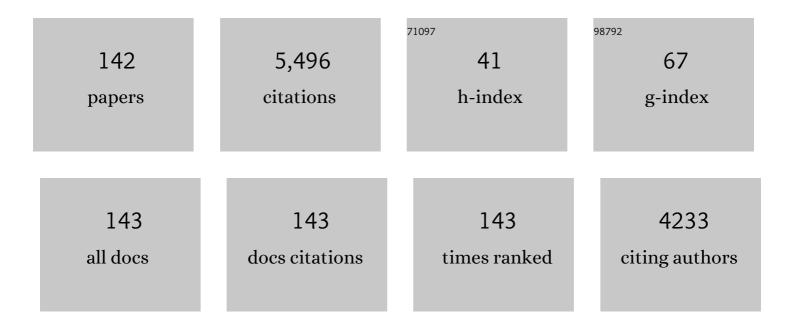
Syed Shatir A Syed-Hassan

List of Publications by Year in descending order

Source: https://exaly.com/author-pdf/2148068/publications.pdf Version: 2024-02-01



#	Article	IF	CITATIONS
1	Thermochemical processing of sewage sludge to energy and fuel: Fundamentals, challenges and considerations. Renewable and Sustainable Energy Reviews, 2017, 80, 888-913.	16.4	428
2	High surface area and mesoporous activated carbon from KOH-activated dragon fruit peels for methylene blue dye adsorption: Optimization and mechanism study. Chinese Journal of Chemical Engineering, 2021, 32, 281-290.	3.5	206
3	Evaluation of the porous structure development of chars from pyrolysis of rice straw: Effects of pyrolysis temperature and heating rate. Journal of Analytical and Applied Pyrolysis, 2012, 98, 177-183.	5.5	189
4	Influence of different demineralization treatments on physicochemical structure and thermal degradation of biomass. Bioresource Technology, 2013, 146, 254-260.	9.6	179
5	Effects of inherent alkali and alkaline earth metallic species on biomass pyrolysis at different temperatures. Bioresource Technology, 2015, 192, 23-30.	9.6	161
6	Evolution of Aromatic Structures during the Low-Temperature Electrochemical Upgrading of Bio-oil. Energy & Fuels, 2019, 33, 11292-11301.	5.1	154
7	Effects of heating rate on the evolution of bio-oil during its pyrolysis. Energy Conversion and Management, 2018, 163, 420-427.	9.2	137
8	Graphene aerogel composites derived from recycled cigarette filters for electromagnetic wave absorption. Journal of Materials Chemistry C, 2015, 3, 11893-11901.	5.5	134
9	Characterization of char from rapid pyrolysis of rice husk. Fuel Processing Technology, 2008, 89, 1096-1105.	7.2	106
10	Mini-Review on Char Catalysts for Tar Reforming during Biomass Gasification: The Importance of Char Structure. Energy & Fuels, 2020, 34, 1219-1229.	5.1	98
11	Pyrolysis of poplar, cellulose and lignin: Effects of acidity and alkalinity of the metal oxide catalysts. Journal of Analytical and Applied Pyrolysis, 2018, 134, 590-605.	5.5	97
12	Assessing the chemical composition of heavy components in bio-oils from the pyrolysis of cellulose, hemicellulose and lignin at slow and fast heating rates. Fuel Processing Technology, 2020, 199, 106299.	7.2	97
13	Steam reforming of acetic acid over Ni/Al2O3 catalysts: Correlation of nickel loading with properties and catalytic behaviors of the catalysts. Fuel, 2018, 217, 389-403.	6.4	95
14	Effects of steam and CO2 on the characteristics of chars during devolatilization in oxy-steam combustion process. Applied Energy, 2016, 182, 20-28.	10.1	93
15	Interaction and kinetic analysis for coal and biomass co-gasification by TG–FTIR. Bioresource Technology, 2014, 154, 313-321.	9.6	90
16	Characteristics and mechanisms of phosphorous adsorption by rape straw-derived biochar functionalized with calcium from eggshell. Bioresource Technology, 2020, 318, 124063.	9.6	90
17	Char Structural Evolution during Pyrolysis and Its Influence on Combustion Reactivity in Air and Oxy-Fuel Conditions. Energy & Fuels, 2012, 26, 1565-1574.	5.1	83
18	Evolution of char structure during steam gasification of the chars produced from rapid pyrolysis of rice husk. Bioresource Technology, 2012, 114, 691-697.	9.6	76

#	Article	IF	CITATIONS
19	Effects of oxygen species from Fe addition on promoting steam reforming of toluene over Fe–Ni/Al2O3 catalysts. International Journal of Hydrogen Energy, 2016, 41, 17967-17975.	7.1	75
20	Investigation of sulfur forms and transformation during the co-combustion of sewage sludge and coal using X-ray photoelectron spectroscopy. Journal of Hazardous Materials, 2009, 167, 1126-1132.	12.4	69
21	Effects of temperature on the yields and properties of bio-oil from the fast pyrolysis of mallee bark. Fuel, 2013, 108, 400-408.	6.4	68
22	Effects of volatile–char interactions on in-situ destruction of nascent tar during the pyrolysis and gasification of biomass. Part II. Roles of steam. Fuel, 2015, 143, 555-562.	6.4	68
23	Effects of reaction conditions on the emission behaviors of arsenic, cadmium and lead during sewage sludge pyrolysis. Bioresource Technology, 2017, 236, 138-145.	9.6	68
24	Carbon nanotubes formation and its influence on steam reforming of toluene over Ni/Al2O3 catalysts: Roles of catalyst supports. Fuel Processing Technology, 2018, 176, 7-14.	7.2	68
25	Microporous activated carbon developed from KOH activated biomass waste: surface mechanistic study of methylene blue dye adsorption. Water Science and Technology, 2021, 84, 1858-1872.	2.5	67
26	Effects of CO2 and heating rate on the characteristics of chars prepared in CO2 and N2 atmospheres. Fuel, 2015, 142, 243-249.	6.4	65
27	Molecular structure characterization of the tetrahydrofuran-microwave-extracted portions from three Chinese low-rank coals. Fuel, 2017, 189, 178-185.	6.4	60
28	H2SO4-treated Malaysian low rank coal for methylene blue dye decolourization and cod reduction: Optimization of adsorption and mechanism study. Surfaces and Interfaces, 2020, 21, 100641.	3.0	60
29	Pyrolysis of the aromatic-poor and aromatic-rich fractions of bio-oil: Characterization of coke structure and elucidation of coke formation mechanism. Applied Energy, 2019, 239, 981-990.	10.1	59
30	Opposite effects of self-growth amorphous carbon and carbon nanotubes on the reforming of toluene with Ni/î±-Al2O3 for hydrogen production. International Journal of Hydrogen Energy, 2017, 42, 14439-14448.	7.1	58
31	Evolution of coke structures during the pyrolysis of bio-oil at various temperatures and heating rates. Journal of Analytical and Applied Pyrolysis, 2018, 134, 336-342.	5.5	57
32	Study on the behavior of heavy metals during thermal treatment of municipal solid waste (MSW) components. Environmental Science and Pollution Research, 2016, 23, 253-265.	5.3	55
33	Process Optimization and Adsorptive Mechanism for Reactive Blue 19 Dye by Magnetic Crosslinked Chitosan/MgO/Fe3O4 Biocomposite. Journal of Polymers and the Environment, 2022, 30, 2759-2773.	5.0	52
34	Steam reforming of acetic acid over Ni/Al2O3 catalyst: Correlation of calcination temperature with the interaction of nickel and alumina. Fuel, 2018, 227, 307-324.	6.4	51
35	Effects of H ₂ O Gasification Reaction on the Characteristics of Chars under Oxy-Fuel Combustion Conditions with Wet Recycle. Energy & Fuels, 2016, 30, 9071-9079.	5.1	50
36	Co-production of hydrogen and carbon nanotubes from the decomposition/reforming of biomass-derived organics over Ni/α-Al2O3 catalyst: Performance of different compounds. Fuel, 2017, 210, 307-314.	6.4	50

#	Article	IF	CITATIONS
37	Promoting effects of Fe-Ni alloy on co-production of H2 and carbon nanotubes during steam reforming of biomass tar over Ni-Fe/α-Al2O3. Fuel, 2020, 276, 118116.	6.4	48
38	Raman Spectroscopy as a Versatile Tool for Investigating Thermochemical Processing of Coal, Biomass, and Wastes: Recent Advances and Future Perspectives. Energy & Fuels, 2021, 35, 2870-2913.	5.1	48
39	Formation, control, and elimination of carbon on Ni-based catalyst during CO2 and CH4 conversion via dry reforming process: A review. Journal of CO2 Utilization, 2022, 61, 102050.	6.8	47
40	Speciation analysis and leaching behaviors of selected trace elements in spent SCR catalyst. Chemosphere, 2018, 207, 440-448.	8.2	45
41	Effect of the pre-reforming by Fe/bio-char catalyst on a two-stage catalytic steam reforming of bio-oil. Fuel, 2019, 239, 282-289.	6.4	45
42	Sulfur self-doped char with high specific capacitance derived from waste tire: Effects of pyrolysis temperature. Science of the Total Environment, 2020, 741, 140193.	8.0	43
43	Formation of the heavy tar during bio-oil pyrolysis: A study based on Fourier transform ion cyclotron resonance mass spectrometry. Fuel, 2019, 239, 108-116.	6.4	42
44	Effects of AAEMs on formation of heavy components in bio-oil during pyrolysis at various temperatures and heating rates. Fuel Processing Technology, 2021, 213, 106690.	7.2	41
45	Kinetic vaporization of heavy metals during fluidized bed thermal treatment of municipal solid waste. Waste Management, 2013, 33, 340-346.	7.4	40
46	Application of Biochar Derived From Pyrolysis of Waste Fiberboard on Tetracycline Adsorption in Aqueous Solution. Frontiers in Chemistry, 2019, 7, 943.	3.6	39
47	Importance of the aromatic structures in volatiles to the in-situ destruction of nascent tar during the volatile–char interactions. Fuel Processing Technology, 2015, 132, 31-38.	7.2	38
48	Effects of the component interaction on the formation of aromatic structures during the pyrolysis of bio-oil at various temperatures and heating rates. Fuel, 2018, 233, 461-468.	6.4	37
49	Optimization of the preparation of activated carbon from palm kernel shell for methane adsorption using Taguchi orthogonal array design. Korean Journal of Chemical Engineering, 2016, 33, 2502-2512.	2.7	36
50	Conversion and transformation of N species during pyrolysis of wood-based panels: A review. Environmental Pollution, 2021, 270, 116120.	7.5	36
51	Temporal and spatial evolution of biochar chemical structure during biomass pellet pyrolysis from the insights of micro-Raman spectroscopy. Fuel Processing Technology, 2021, 218, 106839.	7.2	34
52	Evolution characteristics of different types of coke deposition during catalytic removal of biomass tar. Journal of the Energy Institute, 2020, 93, 2497-2504.	5.3	33
53	Effects of pressure and residence time on limonene production in waste tires pyrolysis process. Journal of Analytical and Applied Pyrolysis, 2020, 151, 104899.	5.5	33
54	Evolution of heavy components during sewage sludge pyrolysis: A study using an electrospray ionization Fourier transform ion cyclotron resonance mass spectrometry. Fuel Processing Technology, 2018, 175, 97-103.	7.2	32

#	Article	IF	CITATIONS
55	Effects of vapor-/solid-phase interactions among cellulose, hemicellulose and lignin on the formation of heavy components in bio-oil during pyrolysis. Fuel Processing Technology, 2022, 225, 107042.	7.2	31
56	Steam reforming of typical small organics derived from bio-oil: Correlation of their reaction behaviors with molecular structures. Fuel, 2020, 259, 116214.	6.4	30
57	Volatile–char interactions during biomass pyrolysis: Cleavage of C–C bond in a β–5 lignin model dimer by amino-modified graphitized carbon nanotube. Bioresource Technology, 2020, 307, 123192.	9.6	30
58	Catalytic pyrolysis of pine wood over char-supported Fe: Bio-oil upgrading and catalyst regeneration by CO2/H2O. Fuel, 2022, 307, 121778.	6.4	30
59	Catalytic Steam Reforming of Biomass-Derived Acetic Acid over Two Supported Ni Catalysts for Hydrogen-Rich Syngas Production. ACS Omega, 2019, 4, 13585-13593.	3.5	29
60	Constructing Co–N–C Catalyst via a Double Crosslinking Hydrogel Strategy for Enhanced Oxygen Reduction Catalysis in Fuel Cells. Small, 2021, 17, e2100735.	10.0	29
61	Formation, fates and roles of catalytic precursors generated from the K2CO3-carbon interactions in the K2CO3-catalyzed CO2 gasification of coal char. Journal of Analytical and Applied Pyrolysis, 2017, 124, 384-392.	5.5	27
62	Performance of Cu-Zn-Al-Zr catalyst prepared by ultrasonic spray precipitation technique in the synthesis of methanol via CO2 hydrogenation. Fuel Processing Technology, 2018, 169, 191-198.	7.2	27
63	Effect of temperature on Shenfu coal pyrolysis process related to its chemical structure transformation. Fuel Processing Technology, 2021, 213, 106662.	7.2	27
64	The synergistic effect of Ca(OH) 2 on the process ofÂlignite steam gasification to produce hydrogen-rich gas. International Journal of Hydrogen Energy, 2014, 39, 15506-15516.	7.1	25
65	A novel sludge pyrolysis and biomass gasification integrated method to enhance hydrogen-rich gas generation. Energy Conversion and Management, 2022, 254, 115205.	9.2	25
66	Mechanistic influences of different solvents on microwave-assisted extraction of Shenfu low-rank coal. Fuel Processing Technology, 2017, 166, 276-281.	7.2	24
67	Study on the structural evolution of semi-chars and their solvent extracted materials during pyrolysis process of a Chinese low-rank coal. Fuel, 2018, 214, 363-368.	6.4	24
68	Direct conversion of furan into levulinate esters via acid catalysis. Fuel, 2019, 237, 263-275.	6.4	24
69	Roles of furfural during the thermal treatment of bio-oil at low temperatures. Journal of Energy Chemistry, 2020, 50, 85-95.	12.9	24
70	NiO reduction with hydrogen and light hydrocarbons: Contrast between SiO2-supported and unsupported NiO nanoparticles. Applied Catalysis A: General, 2011, 398, 187-194.	4.3	23
71	Micro-Raman Spectroscopy Study of 32 Kinds of Chinese Coals: Second-Order Raman Spectrum and Its Correlations with Coal Properties. Energy & Fuels, 2017, 31, 7884-7893.	5.1	23
72	Steam reforming of carboxylic acids for hydrogen generation: Effects of aliphatic chain of the acids on their reaction behaviors. Molecular Catalysis, 2018, 450, 1-13.	2.0	23

#	Article	IF	CITATIONS
73	Structural differences of the soluble oligomers and insoluble polymers from acid-catalyzed conversion of sugars with varied structures. Carbohydrate Polymers, 2019, 216, 167-179.	10.2	23
74	Effect of Ni/Al2O3 mixing on the coking behavior of bio-oil during its pyrolysis: Further understanding based on the interaction between its components. Fuel, 2022, 315, 123136.	6.4	23
75	Hydrogenation of fourteen biomass-derived phenolics in water and in methanol: their distinct reaction behaviours. Sustainable Energy and Fuels, 2018, 2, 751-758.	4.9	22
76	Effect of temperature on multiple competitive processes for co-production of carbon nanotubes and hydrogen during catalytic reforming of toluene. Fuel, 2020, 264, 116749.	6.4	22
77	Catalytic oxidation of ethane with oxygen using fluidised nanoparticle NiO catalyst. Applied Catalysis A: General, 2011, 405, 166-174.	4.3	20
78	Effects of H ₂ O on NO Emission during Oxy-coal Combustion with Wet Recycle. Energy & Fuels, 2017, 31, 8392-8399.	5.1	19
79	Relation between char structures and formation of volatiles during the pyrolysis of Shenfu coal: Further understanding on the effects of mobile phase and fixed phase. Fuel Processing Technology, 2018, 178, 379-385.	7.2	19
80	Pore diameters of Ni/ZrO2 catalysts affect properties of the coke in steam reforming of acetic acid. International Journal of Hydrogen Energy, 2021, 46, 23642-23657.	7.1	19
81	Formation and reduction of NO from the oxidation of NH3/CH4 with high concentration of H2O. Fuel, 2019, 247, 19-25.	6.4	18
82	Performance and Carbonation Kinetics of Modified CaO-Based Sorbents Derived from Different Precursors in Multiple CO2 Capture Cycles. Energy & Fuels, 2016, 30, 9563-9571.	5.1	17
83	Inhibitory effects of CaO/Fe2O3 on arsenic emission during sewage sludge pyrolysis. Bioresource Technology, 2016, 218, 134-139.	9.6	17
84	Identification of the structural characteristics of the asphaltenes in the tetrahydrofuran-microwave-extracted portions from two Chinese coals. Fuel Processing Technology, 2017, 160, 86-92.	7.2	17
85	Insights into evolution mechanism of PAHs in coal thermal conversion: A combined experimental and DFT study. Energy, 2021, 222, 119970.	8.8	17
86	Co-presence of hydrophilic and hydrophobic sites in Ni/biochar catalyst for enhancing the hydrogenation activity. Fuel, 2021, 293, 120426.	6.4	17
87	Functional Mechanism of Inorganic Sodium on the Structure and Reactivity of Zhundong Chars during Pyrolysis. Energy & Fuels, 2017, 31, 10812-10821.	5.1	16
88	Co-hydrothermal carbonization of swine manure and cellulose: Influence of mutual interaction of intermediates on properties of the products. Science of the Total Environment, 2021, 791, 148134.	8.0	16
89	Performance of CaO for phenol steam reforming and water–gas shift reaction impacted by carbonation process. International Journal of Hydrogen Energy, 2015, 40, 13314-13322.	7.1	15
90	Evolution of nitrogen/oxygen substituted aromatics from sludge to light and heavy volatiles. Journal of Cleaner Production, 2020, 257, 120327.	9.3	15

#	Article	IF	CITATIONS
91	Life cycle assessment to evaluate the green house gas emission from oil palm bio-oil based power plant. Korean Journal of Chemical Engineering, 2013, 30, 1277-1283.	2.7	14
92	Experimental study and mechanism analysis of NO formation during volatile-N model compounds combustion in H2O/CO2 atmosphere. Fuel, 2020, 273, 117722.	6.4	14
93	Effect of oxygen concentration on combustion behavior of single coal pellets from three different ranks in a concentrating photothermal reactor. Fuel, 2020, 269, 117372.	6.4	14
94	Roles of calcium oxide on the evolution of substituted polycyclic aromatic hydrocarbons released from sewage sludge pyrolysis. Journal of Cleaner Production, 2021, 317, 128324.	9.3	14
95	Effects of crystallite size on the kinetics and mechanism of NiO reduction with H ₂ . International Journal of Chemical Kinetics, 2011, 43, 667-676.	1.6	13
96	Pyrolysis of herb waste: Effects of extraction pretreatment on characteristics of bio-oil and biochar. Biomass and Bioenergy, 2020, 143, 105801.	5.7	13
97	Roles of dehydration conditioners on the formation of apatite phosphorus during the pyrolysis of various sludge. Journal of Environmental Chemical Engineering, 2021, 9, 105248.	6.7	13
98	Volatile-char interactions during biomass pyrolysis: Insight into the activity of chars derived from three major components. Journal of Analytical and Applied Pyrolysis, 2021, 159, 105320.	5.5	13
99	Co-pyrolysis of swine manure and pinewood sawdust: Evidence of cross-interaction of the volatiles and profound impacts on product characteristics. Renewable Energy, 2021, 179, 1370-1384.	8.9	13
100	Catalytic Steam Reforming of Biomass Tar Model Compound Using Nickel and Cobalt Catalysts Supported on Palm Kernel Shell Char. Journal of Chemical Engineering of Japan, 2016, 49, 29-34.	0.6	12
101	Waste tire heat treatment to prepare sulfur self-doped char via pyrolysis and K2FeO4-assisted activation methods. Waste Management, 2021, 125, 145-153.	7.4	12
102	Polymerization during low-temperature electrochemical upgrading of bio-oil: Multi-technique characterization of bio-oil evolution. Energy Conversion and Management, 2022, 253, 115165.	9.2	12
103	Effect of La-Modified Supporter on H ₂ S Removal Performance of Mn/La/Al ₂ O ₃ Sorbent in a Reducing Atmosphere. Industrial & Engineering Chemistry Research, 2019, 58, 8260-8270.	3.7	11
104	Formation of highly graphitic char derived from phenolic resin carbonization by Ni-Zn-B alloy. Environmental Science and Pollution Research, 2020, 27, 22639-22647.	5.3	11
105	Evolution of coke structures during electrochemical upgrading of bio-oil. Fuel Processing Technology, 2022, 225, 107036.	7.2	11
106	Positive and negative catalytic effects of a nickel mesh catalyst for the partial oxidation of ethane. Chemical Engineering Journal, 2009, 147, 307-315.	12.7	10
107	Evolution of char structure during the pyrolysis of biomass pellet: Further understanding on the effects of chars two phases. Fuel, 2022, 312, 122994.	6.4	10
108	Importance of char-volatiles interactions during co-pyrolysis of polypropylene and biomass components. Journal of Environmental Chemical Engineering, 2022, 10, 108202.	6.7	10

#	Article	IF	CITATIONS
109	High-Efficiency Inhibition of Gravity Segregation in Al–Bi Immiscible Alloys by Adding Lanthanum. Metals and Materials International, 2018, 24, 1262-1274.	3.4	9
110	Effects of the Gas-/Liquid-Phase Interactions on the Evolution of Bio-oil during Its Thermal Treatment. Energy & Fuels, 2020, 34, 8482-8492.	5.1	9
111	One-step preparation of a N-CNTs@Ni foam electrode material with the co-production of H2 by catalytic reforming of N-containing compound of biomass tar. Fuel, 2020, 280, 118601.	6.4	9
112	An insight into the OPAHs and SPAHs formation mechanisms during alkaline lignin pyrolysis at different temperatures. Journal of Analytical and Applied Pyrolysis, 2021, 156, 105104.	5.5	8
113	Comparative study of catalytic and non-catalytic steam reforming of bio-oil: Importance of pyrolysis temperature and its parent biomass particle size during bio-oil production process. Fuel, 2022, 314, 122746.	6.4	8
114	Modification of Iron Oxide to Promote Reaction Property for Chemical Looping Combustion with CO. Combustion Science and Technology, 2016, 188, 1319-1330.	2.3	7
115	Hydrogen-Rich Gas Production from Steam Gasification of Lignite Integrated with CO ₂ Capture Using Dual Calcium-Based Catalysts: An Experimental and Catalytic Kinetic Study. Energy & Fuels, 2018, 32, 1265-1275.	5.1	7
116	Coke formation and its impacts during electrochemical upgrading of bio-oil. Fuel, 2021, 306, 121664.	6.4	7
117	Effects of interactions between organic solid waste components on the formation of heavy components in oil during pyrolysis. Fuel Processing Technology, 2022, 225, 107041.	7.2	7
118	Gasification of Nickel-Preloaded Oil Palm Biomass with Air. Bulletin of Chemical Reaction Engineering and Catalysis, 2016, 11, 262-272.	1.1	6
119	Evolution of Stable Free Radicals during Bio-Oil Pyrolysis and Its Relation to Coke Formation: An in Situ EPR Study. Energy & Fuels, 2022, 36, 7608-7616.	5.1	6
120	Solidification and Leaching Behaviors of V and As in a Spent Catalyst-Containing Concrete. Energy & Fuels, 2020, 34, 7209-7217.	5.1	5
121	Mechanical Characteristics and Energy Consumption of Solid and Hollow Biomass Pellet Production Using a Statistical Analysis of Operating Parameters. Waste and Biomass Valorization, 2021, 12, 6635-6657.	3.4	5
122	Synergistic Removal Effects of Ultralow Emission Air Pollution Control Devices on Trace Elements in a Coal-Fired Power Plant. Energy & Fuels, 2022, 36, 2474-2487.	5.1	5
123	Formation of carbon on non-porous Ni mesh during the catalytic pyrolysis of acetylene. Fuel Processing Technology, 2012, 104, 319-324.	7.2	4
124	Effects of aspect ratio on char structure during the pyrolysis of sawdust pellet. Fuel, 2022, 325, 124850.	6.4	4
125	H2 produced by catalytic reforming of acetic acid over Ni/char catalyst recycled from the biochar adsorption purification of simulated Ni electroplating wastewater. Fuel, 2022, 328, 125243.	6.4	4
126	Preparation and Characterization of Single and Mixed Activated Carbons Derived from Coconut Shell and Palm Kernel Shell through Chemical Activation Using Microwave Irradiation System. Materials Science Forum, 0, 889, 215-220.	0.3	3

#	Article	IF	CITATIONS
127	Experimental Study of Ignition and Combustion Characteristics of Mixed Rice Straw and Sewage Sludge Solid and Hollow Spherical Pellets in a Plasma Combustion System. Key Engineering Materials, 2019, 797, 327-335.	0.4	3
128	Hydrogen- and Methane-Rich Clean Producer Gas from the Reforming of Bio-oil with Fe/AC Catalyst Prepared by a Stepwise Impregnation Method. Bioenergy Research, 0, , 1.	3.9	3
129	METHANE ADSORPTION PERFORMANCE OF THE PALM KERNEL SHELL-DERIVED CARBON MATERIAL ACTIVATED USING CO2-STEAM SEQUENTIAL COMBINATION. Malaysian Journal of Analytical Sciences, 2016, 20, 1390-1397.	0.1	3
130	Coke formation during the pyrolysis of bio-oil: Further understanding on the evolution of radicals. Applications in Energy and Combustion Science, 2022, 9, 100050.	1.5	3
131	Polymerization during low-temperature electrochemical upgrading of bio-oil: Effects of interactions among bio-oil fractions. Energy, 2022, 251, 123944.	8.8	3
132	Roles of inorganic potassium in the evolution of heavy volatile during cellulose steam reforming. Fuel, 2022, 321, 124099.	6.4	3
133	Thermal Behaviour of Slurry Prepared from Clermont Bituminous Coal and Oil Palm Empty Fruit Bunch Bio-Oil. Advanced Materials Research, 2014, 906, 153-158.	0.3	2
134	Effect of Pretreatment on Adsorption of Nickel by Oil Palm Mesocarp Fiber. Advanced Materials Research, 0, 906, 131-136.	0.3	1
135	Adsorption Capacity of Nickel (II) and Cobalt (II) Ions from Aqueous Solutions by Oil Palm Waste and Sawdust. Advanced Materials Research, 0, 911, 322-325.	0.3	1
136	Study on Catalytic Steam Reforming of Toluene over Ni/Activated Carbon Catalysts Prepared from Adsorption Treatment of Nickel Electroplating Wastewater by Activated Carbon. Key Engineering Materials, 0, 797, 92-101.	0.4	1
137	Combustion experimental analysis into effects of interaction between blended coals on the NO emission. IOP Conference Series: Earth and Environmental Science, 0, 657, 012100.	0.3	1
138	Optimization and statistical analysis of the effect of main operation conditions on the physical characteristics of solid and hollow cylindrical pellets. Biomass Conversion and Biorefinery, 0, , 1.	4.6	1
139	Waste Tire Heat Treatment to Prepare Sulfur Self-Doped Char: Operando Insight into Activation Mechanisms Based on the Char Structures Evolution. Processes, 2021, 9, 1622.	2.8	1
140	Fuel properties of bituminous coal and pyrolytic oil mixture. AIP Conference Proceedings, 2014, , .	0.4	0
141	A novel integrated pyrolysis-gasification technology for improving quality of bio-gases from multisource solid wastes. IOP Conference Series: Earth and Environmental Science, 2020, 615, 012063.	0.3	0
142	Effects of Different Physical Activation Agents on Adsorbent Pore Development and Methane Uptake. Recent Innovations in Chemical Engineering, 2022, 15, 127-137.	0.4	0